THE MORPHOLOGICAL ANALYSIS OF CRYSTALLINE METHADONE: A NOVEL COMBINATION OF MICROSCOPY TECHNIQUES

Noor R. Al-Hasani, Paul G. Royall, Neil Rayment, Kim Wolff

The aim: to evaluate combined microscopy techniques for determining the morphological and optical properties of methadone hydrochloride (MDN) crystals.

Materials and methods: MDN crystal formation was optimized using a closed container method and crystals were characterized using polarized light microscope (PLM), scanning electron microscopy (SEM) and confocal microscopy (CM). SEM and CM were used to determine MDN crystal thickness and study its relationship with crystal retardation colours using the Michel-Levy Birefringence approach.

Results: Dimensions (mean±SD) of diamond shaped MDN crystals were confirmed using SEM and CM. Crystals were 46.4±15.2 Vs 32.0±8.3 µm long, 28.03±8.2 Vs 20.85±5.5 µm wide, and 6.62±2.9 Vs 9.6±4.6 µm thick, respectively. There were significant differences between SEM and CM thickness measurements (U=1283, p<0.05), as the SEM exhibited thinner diamond crystals. The combined use of PLM and Michel-Levy chart enabled the observation of a predominantly yellow coloured MDN crystal, mean thickness at (428 nm) mean retardation value.

Conclusion: The SEM was superior and successfully determined MDN crystal dimensions for the first time, whilst the CM results were affected by the Rhodamine dye staining process used for visualisation. The qualitative analysis of the crystallinity status of methadone hydrochloride optimally achieved using a combination of PLM and SEM techniques

Keywords: methadone, birefringence, Michel-Levy birefringence colour chart, recrystallization methods, retardation, 3-D imaging, confocal microscopy, SEM, polarized light microscopy

1. Introduction

Methadone hydrochloride (MDN) is a white crystalline powder, which is soluble in water (12 g/100 mL) and alcohol (8 g/100 mL), and partially insoluble in glycerol and ether [1, 2]. It is an effective pharmacological substitution treatment for opioid dependence. MDN has been adopted in different countries as a maintenance treatment (MMT) for heroin addiction [3–5]. However, MDN can be diverted from legal sources and misused [6–8]. Tablets may be pulverized to powder to be dissolved in water or alcohol for intravenous use or by insufflation [9, 10].

Since MDN is a crystalline opioid [1, 2], microcrystalline tests could have a potential forensic benefit for characterizing illicit sources of the drug. Recommendations to use such tests in characterizing crystalline abused drugs have been advocated for opioids [11, 12]. However, the microcrystalline test provides insufficient data about basic crystal structure of powdered drugs available on the black market [13]. This study investigated whether advanced microscopic techniques could address these issues.

Methadone is an old drug whose crystallisation was last studied in 1950 [14]. MDN crystals were characterised using polarized light microscope (PLM) as diamond in shape with an angle of 62° with 3 refractive indices (α=1.5713, ß=1.6232 and γ=1.6360); indicating that MDN is an anisotropic material [14, 15].

We proposed further work using 3-dimensional examination of MDN crystals with SEM and CM because they have been widely used in pharmaceutical sciences to analyse the morphology of crystalline and controlled drugs [16–18]. Esmaeili, and Khodaei (2019) successfully used SEM and CM in characterizing targeted magnetic nano capsules, which were loaded with MDN and rifampin [19].

To our knowledge the dimensional measurements of MDN crystals, the relationship between the birefringence colours, MDN crystals thickness and the light retardation have not been investigated previously.

The aim of this study was to evaluate the combined microscopic techniques in identifying the morphological and optical properties of MDN crystals for use in forensic investigations to identify unknown powders in forensic cases.

2. Planning(methodology) of the research

To achieve the goal of this study the following stages were followed:

– Stage I – MDN crystallization optimization stage: in which, three different methods for preparing methadone crystals were used to elect the best one that could be used to prepare a satisfactory amount of MDN crystals depending on the physical properties of MDN powder.

– Sage II – Characterisation stage: here the produced crystals was characterised by different microscopic techniques depending on the MDN crystals optical properties.

– Stage III – The microscopic-linked readings stage: in this stage the results obtained from stage II were linked to establish a novel approach for characterising MDN crystals considering all the pros and cons of this method. This stage was based on employing the inherent optical properties of MDN crystals (refractive indices and birefringence colours) in correlation with MDN crystal thickness to better characterise MDN crystals.

3. Materials and methods
3. 1. Materials

Methadone hydrochloride ≥98 % (MWT 345.91, Lot# SLBC6135V) and HPLC grade water (MWT 18.02, Lot# BCBR 0209V) were purchased from Sigma-Aldrich Company (Gillingham, UK). Gilson's pipettes (Pipetman 2–20 μL) and (Pipetman 100–100 μL) were purchased from Gilson Scientific Limited (Bedfordshire, UK). The polarized light microscope Leitz Dialux 22EB: Leica Microsystems UK Ltd, Milton Keynes, the Leica confocal microscope (TCS-SP2, Wetziar, Germany) and the SEM (Hitachi S 4000 F.E.G., Tokyo, Japan) were used for morphological characterization. For MDN particle size measurements, the optical microscope (Nikon Labophoto) with the Panasonic camera (WVCL310) and the particle size analysis software (V1999) were used. The temperature and humidity were measured by Datalogger, USB, Temp/RH (catalogue number is IN07645) purchased from Lascar company (Wiltshire, UK). Rhodamine B dye (Lot# 47H3506) purchased from Sigma-Aldrich, Gillingham, UK. Image J software (1.50i/ national institute of health USA). Hot-plate stirrer (Harmony HTS-1003) was purchased from Yorlab company, York, UK). For statistical comparisons, the SPSS 24 software was used.

3. 2. Methods
3. 2. 1. Optimization of MDN re-crystallisation

To optimize MDN re-crystallisation, MDN powder was mixed with HPLC grade water. Room temperature and humidity were recorded using USB datalogger. Three different techniques were explored:

1. Weighed MDN method: glass microscope slides were prepared in a ratio of 1:4 (MDN:water). MDN (2.5 mg) was spread onto the slide with 10 μL of HPLC water.

2. Hot stage method: MDN solution (10 μL of HPLC water and MDN 2.5 mg) was covered with a coverslip and sealed to prevent evaporation. The slide was heated to 50 °C (rate of 1 °C/min) with a holding time of 10 mins at this temperature. Undissolved particles of the super saturated solution of MDN was used for the crystallisation process. The heating and cooling cycles were observed using the PLM (Dialux 22EB, Leitz) and the Qi Imaging camera with a magnification of X25.

3. Closed container method: MDN solution (50 mg MDN mixed 200 μL of HPLC water at 50 °C) in a closed vial (n=2), vortexed for 10s and cooled down for 2 hrs to 3.5 °C. MDN crystal formation from each vial (10 μL on a microscope slide) was observed by PLM.

3. 2. 2. Polarized light microscope (PLM) observation method

The PLM was used to study the optical properties of MDN particles and crystals and to determine retardation colours. The prepared slides of MDN-water solutions were observed using the PLM (Dialux 22EB, Leitz) and the Qi Imaging camera with a magnification of X25. For polarized observations a cross-polarizing filter and λ (Lambda) plate red 1 compensator were used to enhance the contrast images quality [20]. The cross polarizer was rotated until the extinction position was achieved (black background obtained) to make a contrast between the sample crystals and the slide background [20, 21]. To investigate the effect of the cross-polarizer angle setting on the retardation colour of MDN particles, 0.25 mg of MDN powder was spread on a microscope slide and observed by the PLM. For standardization, delineation of the central area (25×20 mm) of the bottom side of the slide was carried out using a permanent marker. Then, this area was dynamically observed (from the top side where the methadone hydrochloride powder is distributed) with a magnification of ×40.

3. 2. 3. Characterizing MDN particles

The optical microscope (Nikon Labophoto) with a Panasonic camera (WVCL310) and particle size analysis software (V1999) were used to observe 3 slides of MDN (magnification of X40) to measure the particle size of 500 MDN particles by measuring the volume diameter. The volume diameter was defined as the volume of a sphere having the same volume as the particle, and it was calculated according to equation (1):

$$dv = \left(6v / \pi\right)^{1/3}, \qquad (1)$$

where dv – volume diameter, and v –volume of the particle.

An anisotropic material such as MDN has more than one refractive index (RI or n) depending upon the lattice direction; the difference between the RIs (Δn) of the material is known as birefringence [21–23].

3. 2. 4. Scanning electron microscope observations

The SEM was previously used to characterize crystal morphology at room temperature [17, 24]. MDN Crystals were prepared using the closed container method for SEM observations. PLM observations were carried out using a magnification of X25 before gold coating to correlate MDN crystals colours with the thickness measurements. Each slide was metallised with gold (15 nm thickness) using a method described by [25]. Totally, 42 crystals were observed (Six crystals for 7 slides) using SEM at an accelerating voltage of 20 kV [26]. The crystal dimension measurements were carried out in duplicate using Quartz PC software using an aerial image to determine length and width measurements, and a ver-

tical view (90° tilting) to measure the thickness of each crystal.

3. 2. 5. Confocal microscope observations

The confocal microscope generated a 3D image by scanning the optical sections of the sample using Z-stack scan, which is a digital image processing technique providing three-dimensional views [18, 27, 28]. The Z-stack scanning technique was used to determine if the CM could measure crystal dimensions including its thickness [28, 29].

CM samples were prepared as follows: MDN solution (closed container method) required 0.0001 % g/mL warm rhodamine (Rh) solution (50 °C) as a crystallising solvent for the confocal microscopy. The Rh solution (0.0001 % gm/mL) was prepared by mixing 0.1 g of rhodamine dye with 100 mL of HPLC water. Then 1 mL of Rh solution (0.1 % g/mL) was diluted to a 0.0001 % g/mL solution. Seven slides were prepared, and 6 crystals were observed from each slide ($n=42$). The confocal images used a magnification of ×40 at excitation level 543 nm.

3. 3. Statistical analysis

MDN crystals ($n=42$) were analysed to determine the crystal length, width, and thickness using SPSS 24 software. Independent samples t-test and Mann-Whitney U test were used to carry out the inferential statistics between the SEM and CM measurements. The mean values of MDN crystals thickness were measured and used in the following equation:

$$\text{Retardation } (r)=\text{thickness } (t)\times\text{birefringence.} \qquad (2)$$

As the thickness was measured in μm, the retardation was usually measured in nm, and the birefringence represented the difference between the biggest and smallest refractive indices ($n2$ and $n1$ respectively). The equation that was used to calculate the retardation was [21]:

$$r=1000\times t\times(n2-n1). \qquad (3)$$

After obtaining the mean values of retardation, the prediction of the birefringence colours range of MDN crystals was obtained using Michel-Levy Birefringence Chart.
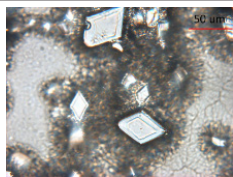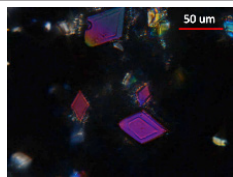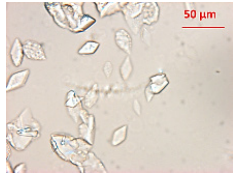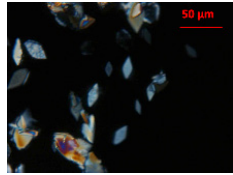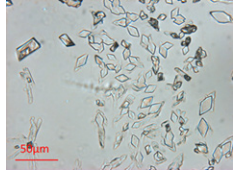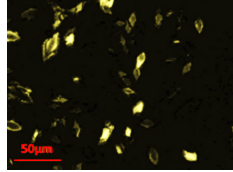
4. Results

Satisfactory MDN crystallisation was recorded for the closed container method: single diamond shaped MDN crystals were formed with the lowest MDN crystalline aggregation as compared with the other methods. During the MDN re-crystallisation process, the relative humidity (% RH) was found to impact on MDN re-crystallisation. Although between 24 % and 70 % RH, satisfactory MDN crystal formation was achieved using the closed container-method. However, when the RH>70 % no MDN crystal were produced. Room temperature changes did not alter the MDN re-crystallising or characterization process. The polarized and non-polarized photomicrographs of re-crystallised MDN using the closed container method showed better consistency of shape and number of crystals formed. The crystals were diamond in shape and exhibited yellow

retardation colours (Table 1). Therefore, the closed container method was shown to outperform other methods and, hence, was used in all further experimentations.

Table 1

Polarized photomicrographs of MDN crystals (with a magnification of X25) prepared with HPLC water using slides methods showing different retardation colours exhibited by MDN diamond crystals

Crystal preparation method	Unpolarized photomicrograph	Polarized photomicrograph (aggregations image)
Weighed MDN method		
Saturated solution of MDN (Hot method using hot stage)		
Saturated solution of MDN (using closed container method)		

MDN crystal preparations yielded a diamond shape as demonstrated in the orthographic projection (Fig. 1), which shows an intrinsic angle of 62°.
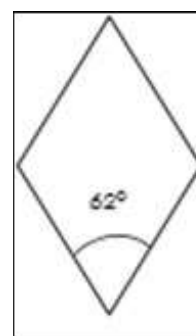

Fig. 1. Orthographic projection of a MDN crystal, showing the diagnostic angle of 62° for MDN crystals

Characterization of MDN crystals using SEM and CM.

The dimensions of MDN crystals determined by using SEM and CM. SEM images of MDN crystals at 90º tilting of the slide enabled the determination of the thickness of the crystals in μm (Fig. 2). Six single crystals separated per slide were eligible for 3D imaging using the SEM.

In the top view (Fig. 2, *a, c, e*) the longest dimension represented the crystal length, while the shortest represented MDN crystal width. Three further SEM images of MDN crystals (Fig. 2, *b, d, f*) at 90° tilting position demonstrate

the thickness measurements of these crystals. Using an aerial view of MDN crystal, the mean length of MDN crystal was 46.4±15.2 µm (range 12.6 µm to 83.3 µm), whilst the width was 28.03±8.2 µm (range 9.0 µm to 45.8 µm), and the thickness 6.62±2.9 µm (range 3 µm to 12.9 µm). It was also possible to measure the dimensions of MDN crystals using the CM (Fig. 3). These pictures show the aerial view and the 3D view of MDN crystals. The confocal microscope visually divided each crystal to several slices and measured the thickness by the z-stack technique.
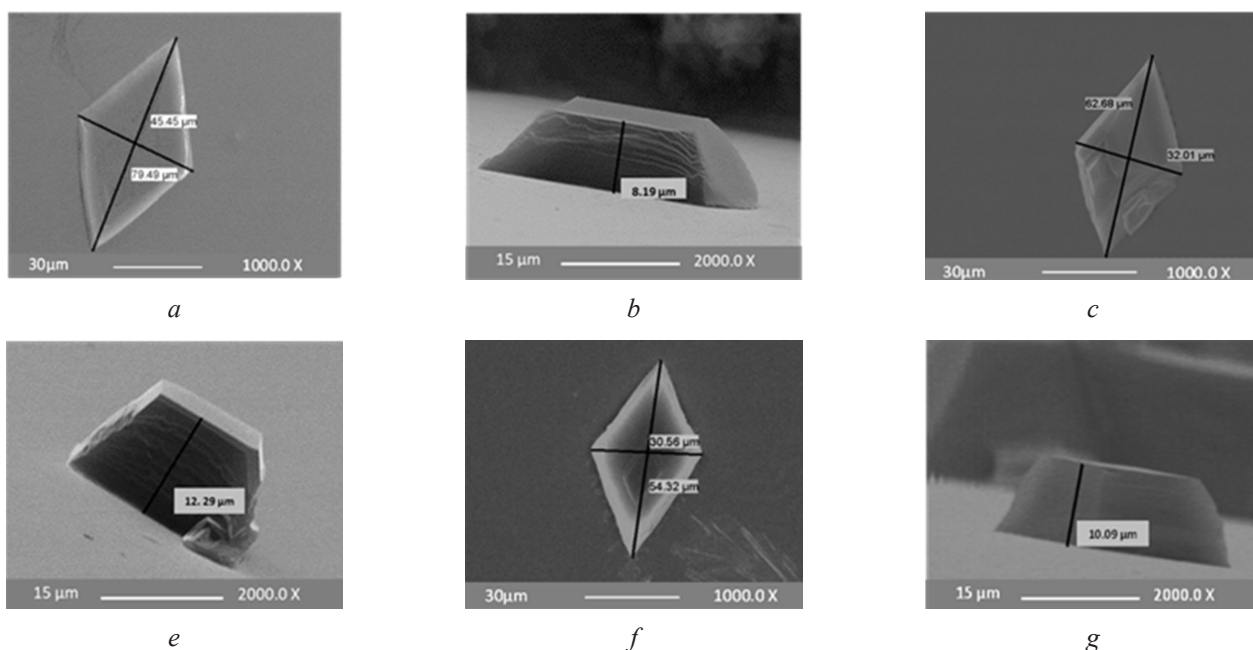

Fig. 2. Length, width, and thickness measurements of MDN crystals: *a, c, e* – SEM images of aerial views for MDN crystals length and width; *b, d, f* – thickness measurements of MDN crystals
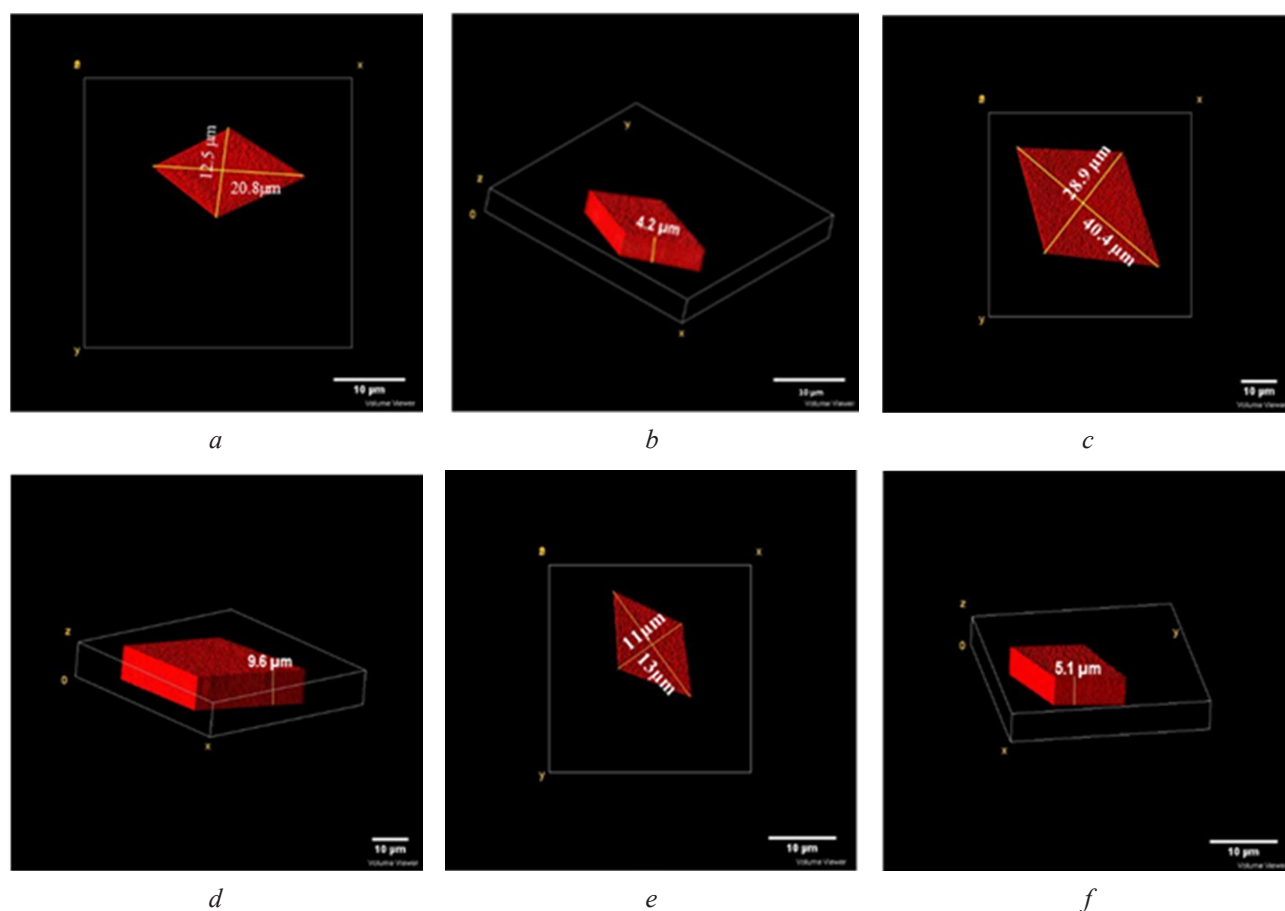

Fig. 3. Confocal microscope images of MDN crystals (magnification of ×40), showing the dimension values of MDN crystals: *a, c, e* – the aerial views of MDN crystals length and width; *b, d, f* – thickness measurements of MDN crystals. MDN crystals exhibited a red colour because of rhodamine B dye

The mean MDN crystal length was 32.0±8.3 µm (range 13.5 µm – 52.52 µm), the width 20.85±5.5 µm (range 8.08 µm – 32.13 µm), and the thickness 9.6±4.6 µm (range 4.2 µm to 24.38 µm). Significant differences were observed when SEM and CM MDN crystal dimensions were compared. SEM MDN crystals were significantly longer (t (82)=5.14, $p<0.05$) and wider (t (82)=4.72, $p<0.05$) than CM dimensions (mean length of 46.4±15.2 µm versus 32±8.3 µm, and mean width of 28.03±8.2 µm versus 20.85±5.5 µm, respectively). An independent samples Mann-Whitney U Test showed SEM MDN crystals significantly thinner (U=1283, $p<0.05$) than CM crystals (6.62±2.9 µm Vs 9.6±4.6 µm).

The retardation range for MDN crystal thickness (measured by SEM) was 195 - 839 nm. The mean SEM thickness of MDN crystals was 6.62 µm, yielding a retardation value at 428 nm (Fig. 4). According to the Michel- Levy birefringence colour chart, therefore most MDN crystals should demonstrate a yellow colour (at the extinction position) as seen in the PLM photomicrographs in Table 1.
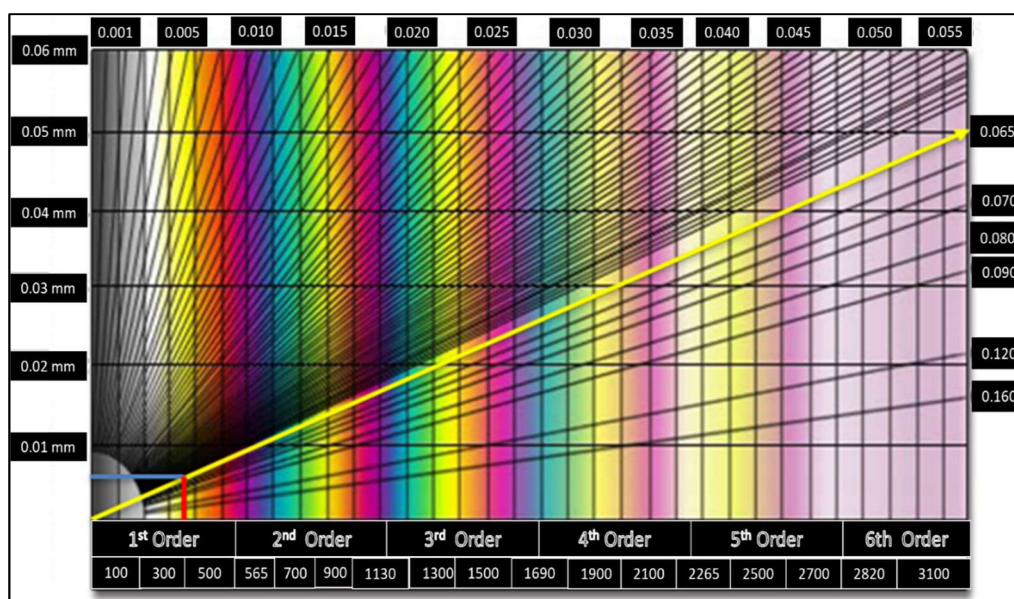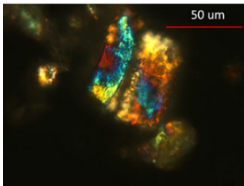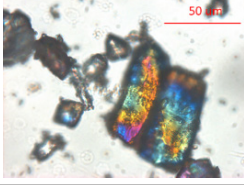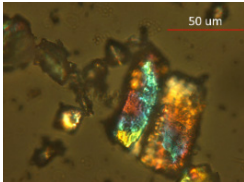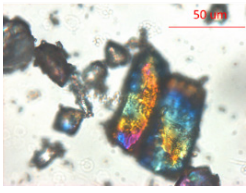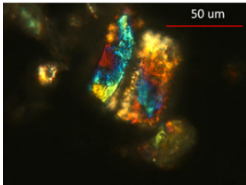

Fig. 4. Michel- Levy birefringence colour chart, demonstrating the retardation value of MDN crystal thickness according to the SEM measurements. By intersecting the diagonal line starting from 0.065 (yellow line) with blue line at 6.62 µm (the mean value of MDN crystals thickness) and drawing the red line perpendicular on the x-axis, the retardation value would be at about 428 nm

Table 2

Photomicrographs of MDN particles at the extinction position and after clockwise rotation of the cross polarizer at different positions

Cross polarizer position	Polarized photomicrograph	Observations
1	2	3
At the extinction position		Interference colours were observed for MDN particles as they exhibited different colours such as yellow, green, red, and orange. Black background denotes what is known as extinction position
After 90° clockwise rotation		The interference colours of MDN particles were changed as compared with the interference colours of MDN particles at the extinction position. For example, the green areas of MDN particles turned to orange after 90°clockwise rotation of the cross polarizer
After 180° clockwise rotation		At 180° interference colours of MDN particles were different as compared with the interference colours of MDN particles at the previous positions. For example, there were bright blue areas of MDN particles (which were noticed at the previous position) turned to orange colour areas at this position

Continuation of Table 2

1	2	3
After 270° clockwise rotation		At 270° interference colours changed as compared with the interference colours of MDN particles at the extinction position; however, the same interference colours of MDN particles noticed at 90°of the clockwise rotation were recorded
After 360° clockwise rotation		After 360° clockwise rotation, the same interference colours were obtained at the extinction position as previously observed

MDN particle were found to range from 2.1 to 44.0 µm with a mean projected area diameter of 26.6±1.8µm. The descriptive analyses of MDN particle size measurements are illustrated in Fig. 5. Micro particles and very fine particles were identified alongside MDN crystals. The micro particles represented 25.7 % of the powder with a volume diameter ranging from 0.1 to 10 µm, while the bulk weight of the powder had a volume diameter ranging from 28.7 to 45.4 µm (classified as very fine particles).

The cross polarizer setting effects on the retardation colours of MDN particles were studied and the photomicrographs of MDN particles at different cross polarizer positions in relation to the extinction position could be seen in Table 2. In addition to the colour change observations, some of MDN particles were no longer visible at the extinction position, while they can be seen at other positions of the cross polarizer (Table 2).
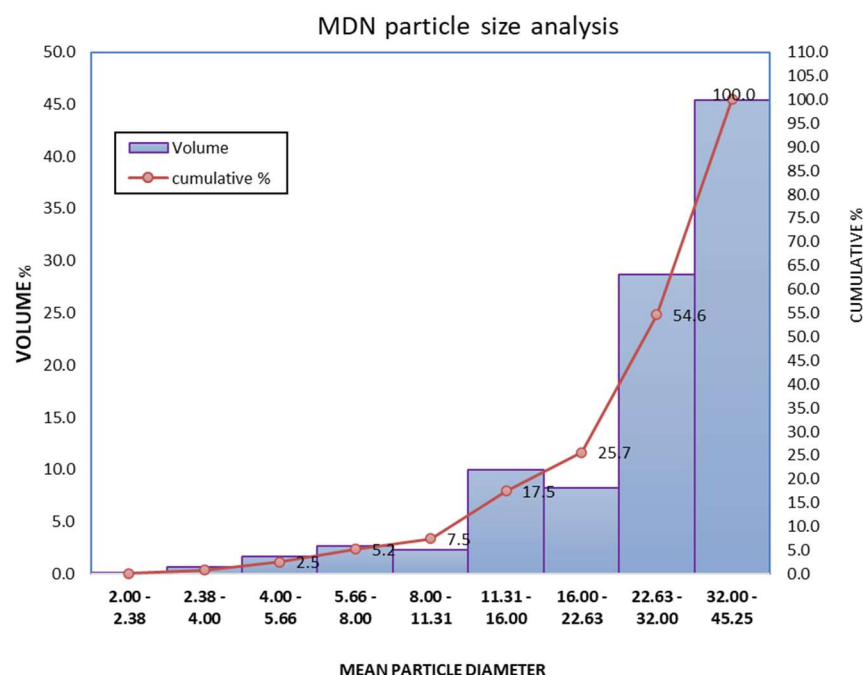

Fig. 5. MDN particle size analysis, showing two series of data: the blue one represents the volume diameter of MDN particles, and the orange series represents the cumulative percentages. More than fifty percent of the particles had volume diameter equal or less than 28.7 µm

5. Discussion

This study established the optimal conditions and methods needed to prepare and characterize MDN crystals using different microscopic techniques. MDN crystal thickness, birefringence colour and retardation relationship were established for the first-time using Michel-Levy birefringence colour chart.

In accordance with Hubach and Jones original work, water was used as an inexpensive, safe, easy to use solvent. MDN recrystallisation was optimized by slow heating and cooling the supersaturated MDN solution in a closed container. An important finding was the impact of humidity >70 % on MDN recrystallisation. Mullin (2001) has noted that nucleation and crystal growth rate can be affected in this way [30].

The PLM continues to be the best tool for characterizing anisotropic materials and crystalline drugs [14, 20, 22] such as methadone. We confirmed the formation of the typical diamond shaped MDN crystal with 62° angle value.

Different retardation colours were shown with the PLM such as purple, blue and yellow. This was attributed to the effect of the anisotropic material (MDN) on the polarized light as when white light passed through the polarizer, the MDN travelling at different velocities (acting as a beam splitter), splits the plane polarized light into two parts, each one vibrating in two separate planes perpendicular to each other (ordinary and extraordinary rays). One ray is retarded in respect to the other (this optical condition is known as retardation). When the ordinary and extraordinary rays pass through the analyzer, they interfere or recombine causing the specimen to appear coloured [31]. Thus, optical interference at the analyzer plane, which destroys some wavelengths and reinforces others [15, 20, 21], is behind the appearance of different colours of MDN crystals and particles.

49

In addition, the appearance of different MDN crystal and particle colours may be attributed to the difference in MDN sample thickness, as sample thickness and retardation values affect the appearance of interference colours [21, 32]. Differentiation of the interference colours of MDN crystals was achieved by identifying the range of MDN crystals thickness, and correlating the retardation, thickness, and birefringence of anisotropic crystals (equation (2)). This outcome, coupled with the aid of Michel-Levy birefringence colour chart, can help to enrich the pharmaceutical and forensic database about MDN crystals characterization.

It was also observed that the analyzer-polarizer angle affected the retardation colours of MDN particles. This was due to the creation of different wavelength interferences of the polarized light that passed through the anisotropic material (MDN) at the analyzer level, producing different interference colours at 90°, 180°, and 270° as compared to the interference colours at the extinction position. Therefore, MDN particle colours change if the angle between the polarizer and the analyzer was altered. Hence, to standardize the diagnosis of MDN for forensic purposes, MDN particles and crystals should be observed at the extinction position when the cross polarizers are perpendicular to each other.

Some MDN particles that did not exhibit interference colours (or appeared black) at the extinction site can be attributed to the fact that the direction of one of the principal refractive indices was parallel to the vibration direction of the polarizer. This led to cancellation of the second vector component; therefore, the second vector equalled zero. In this case, the emerging light from the material had the same vibration direction as the polarizer, i.e., the emerging light direction was perpendicular to the analyzer direction. Thus, the analyzer absorbed the emerging light and prohibited its transformation on to the microscope objectives leading to the appearance of black spots [21, 33].

The rotary stage of the SEM enabled the determination of the actual dimensions of MDN crystals in a standard manner using the tilting procedure at 90°. A MDN crystal was confirmed as diamond shaped with an intrinsic angle of 62°, mean length 46.4±15.2 µm, width 28.03±8.2 µm and thickness of 6.62±2.9 µm. However, the mandatory gold coating step meant that this diagnostic test is expensive and requires trained personnel in addition to the difficulties of the tilting procedure to 90°, encouraged the trial of an alternative technique.

The CM using Rhodamine B dye to characterize MDN could determine dimensions using horizontal (x, y) imaging over a wide area of a crystal, and Z-stacks to determine sample thickness [34]. MDN re-crystallisation with warm super saturated rhodamine solution helped to overcome the disadvantages mentioned by Singh et al. in 2012 [18] in providing a more uniform staining of MDN crystals, but there was a difficulty in measuring the thickness accurately and significant differences in the dimensions measured using Z-stack scanning. This was attributed to the imaging process requiring emitted light from the stained MDN crystals. The poorer resolution of dimensions achieved by the effect of rhodamine B dye accounted for the significant difference between SEM and CM dimensions for MDN crystals. CM was shown to be less reliable in measuring MDN crystals than the SEM.

The demonstration of a correlation between the thickness of a MDN crystal and the retardation value of MDN using the Michel-Levy birefringence chart helped to explain the range of retardation colours exhibited by MDN crystals under the PLM. Moreover, the predominant yellow colour of MDN crystals observed by using the PLM reflected the retardation value of MDN crystals with a mean thickness of 6.62±2.9 µm. This was confirmed by the mathematical calculation thus confirming the colour yellow as a defining characteristic of the MDN crystal.

Besides confirming the colours range of MDN crystals, the Michal-Levy birefringence chart was embodied in the determination of retardation value for MDN crystals. In a previous study, Beaufort et al. (2014) calculated the thickness of calcite crystals using PLM (with a cross polarizer) in relation to the Michal-Levy birefringence colour chart. However, they could not verify the crystal thickness when greater than 4.5 µm [35] and reported this as a limitation for the PLM; a shortcoming confirmed in our study. In contrast, using SEM thickness measurements of MDN crystals with the aid of Michel-Levy birefringence colour chart, MDN crystals retardation colour range was successfully determined to be between 195–839 nm.

The success of determining a procedure to characterize MDN crystals may be encouraging in terms of application to other types of controlled crystalline drugs with the potential usefulness in forensic cases to identify powders of unknown sources, particularly new psychoactive substances (NPS).

Study limitations. The number of measured crystals was limited to 42 crystals due to the technical difficulties and high cost required for measuring MDN crystals thickness using the SEM. In addition, more crystalline addictive drugs should have been studied to establish a library of crystalline addictive drugs that could be used in identifying the unknown powders of these materials.

Prospects for further research. Studying the cooling and time effects on the MDN crystallisation process as they are important parameters that can influence MDN crystals formation.

1. Studying the efficacy of these techniques in characterizing methadone hydrochloride crystals that can be prepared from crushed tablets.

2. Establishing the relationship between MDN birefringence colours, crystal thickness and the Michael-Levey birefringence colour chart using the SEM to establish a diagnostic method for detecting the source or the supplier of MDN.

6. Conclusion

The closed container method was best to re-crystallise MDN at room temperature with relative humidity <70 % RH. This procedure produced recognised diamond shaped crystal, with a diagnostic angle of 62°. Thickness of MDN crystal and the refractive indices

were contributing factors to the resultant retardation colour, expected to be yellow.

Due to the ambiguous correlation between the birefringence theory and the properties of MDN crystals, a combined use of microscopic techniques was developed and correlated for the first time using the SEM that the mean values for a single MDN crystal length (46.4±15.2 μm), width (28.03±8.2 μm) and thickness (6.62±2.9 μm).

Conflict of interest

The authors declare that they have no conflict of interest in relation to this research, whether financial, personal, authorship or otherwise, that could affect the research and its results presented in this paper.

References

1. Bishara, R. H. (1974). Methadone Hydrochloride. Analytical Profiles of Drug Substances. Vol. 3. Academic Press, 365–439. doi: http://doi.org/10.1016/s0099-5428(08)60074-x

2. Moffat, A. C., Osselton, M. D., Widdop, B., Watts, J. (2019). Clarke's analysis of drugs and poisons. Vol. 3. London: Pharmaceutical press.

3. Pan, P.-P., Wang, J., Luo, J., Wang, S.-H., Zhou, Y.-F., Chen, S.-Z., Du, Z. (2017). Silibinin affects the pharmacokinetics of methadone in rats. Drug Testing and Analysis, 10(3), 557 –561. doi: http://doi.org/10.1002/dta.2235

4. Sun, H.-M., Li, X.-Y., Chow, E. P. F., Li, T., Xian, Y., Lu, Y.-H. et. al. (2015). Methadone maintenance treatment programme reduces criminal activity and improves social well-being of drug users in China: a systematic review and meta-analysis. BMJ Open, 5 (1), e005997–e005997. doi: http://doi.org/10.1136/bmjopen-2014-005997

5. Russolillo, A., Moniruzzaman, A., Somers, J. M. (2018). Methadone maintenance treatment and mortality in people with criminal convictions: A population-based retrospective cohort study from Canada. PLOS Medicine, 15 (7), e1002625. doi: http://doi.org/10.1371/journal.pmed.1002625

6. Bretteville-Jensen, A. L., Lillehagen, M., Gjersing, L., Andreas, J. B. (2015). Illicit use of opioid substitution drugs: Prevalence, user characteristics, and the association with non-fatal overdoses. Drug and Alcohol Dependence, 147, 89–96. doi: http://doi.org/10.1016/j.drugalcdep.2014.12.002

7. Harris, M., Rhodes, T. (2013). Methadone diversion as a protective strategy: The harm reduction potential of "generous constraints." International Journal of Drug Policy, 24 (6), e43–e50. doi: http://doi.org/10.1016/j.drugpo.2012.10.003

8. Winstock, A. R., Lea, T. (2009). Diversion and Injection of Methadone and Buprenorphine Among Clients in Public Opioid Treatment Clinics in New South Wales, Australia. Substance Use & Misuse, 45 (1-2), 240–252. doi: http://doi.org/10.3109/10826080903080664

9. Betancourt, A. O., Gosselin, P. M., Vinson, R. K. (2012). New immediate release formulation for deterring abuse of methadone. Pharmaceutical Development and Technology, 18 (2), 535–543. doi: http://doi.org/10.3109/10837450.2012.680598

10. Shaw, I. F., Berk, J. (1976). U.S. Patent No. 3,980,766. Washington: U.S. Patent and Trademark Office; published: 14.09.1976.

11. Elie, L. E., Baron, M. G., Croxton, R. S., Elie, M. P. (2012). Investigation into the suitability of capillary tubes for microcrystalline testing. Drug Testing and Analysis, 5 (7), 573–580. doi: http://doi.org/10.1002/dta.1372

12. Elie, L., Baron, M., Croxton, R., Elie, M. (2012). Microcrystalline identification of selected designer drugs. Forensic Science International, 214 (1-3), 182–188. doi: http://doi.org/10.1016/j.forsciint.2011.08.005

13. Kuś, P., Rojkiewicz, M., Kusz, J., Książek, M., Sochanik, A. (2019). Spectroscopic characterization and crystal structures of four hydrochloride cathinones: N-ethyl-2-amino-1-phenylhexan-1-one (hexen, NEH), N-methyl-2-amino-1-(4-methylphenyl)-3-methoxypropan-1-one (mexedrone), N-ethyl-2-amino-1-(3,4-methylenedioxyphenyl)pentan-1-one (ephylone) and N-butyl-2-amino-1-(4-chlorophenyl)propan-1-one (4-chlorobutylcathinone). Forensic Toxicology, 37 (2), 456–464. doi: http://doi.org/10.1007/s11419-019-00477-y

14. Hubach, C. E., Jones, F. T. (1950). Methadone Hydrochloride Optical Properties, Microchemical Reactions, and X-Ray Diffraction Data. Analytical Chemistry, 22 (4), 595–598. doi: http://doi.org/10.1021/ac60040a028

15. Bibi, S., Kaur, R., Henriksen-Lacey, M., McNeil, S. E., Wilkhu, J., Lattmann, E. et. al. (2011). Microscopy imaging of liposomes: From coverslips to environmental SEM. International Journal of Pharmaceutics, 417 (1-2), 138–150. doi: http://doi.org/10.1016/j.ijpharm.2010.12.021

16. Kölemek, H., Bulduk, İ., Ergün, Y., Konuk, M., Korcan, S. E., Liman, R., Çoban, F. K. (2019). Synthesis of Morphine Loaded Hydroxyapatite Nanoparticles (HAPs) and Determination of Genotoxic Effect for Using Pain Management. Journal of Pharmaceutical Research International, 25 (6), 1–13. doi: http://doi.org/10.9734/jpri/2018/v25i630116

17. Kania, A., Talik, E., Szubka, M., Ryba-Romanowski, W., Niewiadomski, A., Miga, S., Pawlik, M. (2016). Characterization of Bi2WO6 single crystals by X-ray diffraction, scanning electron microscopy, X-ray photoelectron spectroscopy and optical absorption. Journal of Alloys and Compounds, 654, 467–474. doi: http://doi.org/10.1016/j.jallcom.2015.09.127

18. Singh, M. R., Chakraborty, J., Nere, N., Tung, H.-H., Bordawekar, S., Ramkrishna, D. (2012). Image-Analysis-Based Method for 3D Crystal Morphology Measurement and Polymorph Identification Using Confocal Microscopy. Crystal Growth & Design, 12 (7), 3735–3748. doi: http://doi.org/10.1021/cg300547w

19. Khodaei, M., Esmaeili, A. (2019). New and Enzymatic Targeted Magnetic Macromolecular Nanodrug System Which Delivers Methadone and Rifampin Simultaneously. ACS Biomaterials Science & Engineering, 6 (1), 246–255. doi: http://doi.org/10.1021/acsbiomaterials.9b01330

20. Warren, F. J., Royall, P. G., Butterworth, P. J., Ellis, P. R. (2012). Immersion mode material pocket dynamic mechanical analysis (IMP-DMA): A novel tool to study gelatinisation of purified starches and starch-containing plant materials. Carbohydrate Polymers, 90 (1), 628–636. doi: http://doi.org/10.1016/j.carbpol.2012.05.088

21. Jaffe, M., Hammond, W., Tolias, P., Arinzeh, T. (Eds.). (2012). Characterization of biomaterials. Elsevier, 344.

22. Carlton, R. A. (2011). Polarized Light Microscopy. Pharmaceutical microscopy. Springer Science & Business Media, 7–64. doi: http://doi.org/10.1007/978-1-4419-8831-7

23. Frandsen, A. F. (2016). Polarized light microscopy (No. KSC-E-DAA-TN37401).

24. Klang, V., Valenta, C., Matsko, N. B. (2013). Electron microscopy of pharmaceutical systems. Micron, 44, 45–74. doi: http://doi.org/10.1016/j.micron.2012.07.008

25. Ren, F., Su, J., Xiong, H., Tian, Y., Ren, G., Jing, Q. (2016). Characterization of ibuprofen microparticle and improvement of the dissolution. Pharmaceutical Development and Technology, 22 (1), 63–68. doi: http://doi.org/10.3109/10837450.2016.1163386

26. Wei, L., Yang, Y., Shi, K., Wu, J., Zhao, W., Mo, J. (2016). Preparation and Characterization of Loperamide-Loaded Dynasan 114 Solid Lipid Nanoparticles for Increased Oral Absorption In the Treatment of Diarrhea. Frontiers in Pharmacology, 7. doi: http://doi.org/10.3389/fphar.2016.00332

27. Furrer, P., Gurny, R. (2010). Recent advances in confocal microscopy for studying drug delivery to the eye: Concepts and pharmaceutical applications. European Journal of Pharmaceutics and Biopharmaceutics, 74 (1), 33–40. doi: http://doi.org/10.1016/j.ejpb.2009.09.002

28. Prasad, V., Semwogerere, D., Weeks, E. R. (2007). Confocal microscopy of colloids. Journal of Physics: Condensed Matter, 19 (11), 113102. doi: http://doi.org/10.1088/0953-8984/19/11/113102

29. Korlach, J., Schwille, P., Webb, W. W., Feigenson, G. W. (1999). Characterization of lipid bilayer phases by confocal microscopy and fluorescence correlation spectroscopy. Proceedings of the National Academy of Sciences, 96 (15), 8461–8466. doi: http://doi.org/10.1073/pnas.96.15.8461

30. Mullin, J. W. (2001). Crystallization. Elsevier. doi: http://doi.org/10.1016/b978-0-7506-4833-2.x5000-1

31. Agio, M., Alù, A. (Eds.). (2013). Optical antennas. Cambridge University Press. doi: http://doi.org/10.1017/cbo9781139013475

32. Houck, M. M., Siegel, J. A. (2015). Friction ridge examination. Fundamentals of forensic science. San Diego: Elsevier Ltd, 493–518. doi: http://doi.org/10.1016/b978-0-12-800037-3.00019-4

33. Patzelt, W., Leitz, E. (1985). Polarized Light Microscopy-Principles. Instruments, Applications. Wetzlar: Ernst Leitz Wetzlar GmbH, 103.

34. Pygall, S. R., Whetstone, J., Timmins, P., Melia, C. D. (2007). Pharmaceutical applications of confocal laser scanning microscopy: The physical characterisation of pharmaceutical systems. Advanced Drug Delivery Reviews, 59 (14), 1434–1452. doi: http://doi.org/10.1016/j.addr.2007.06.018

35. Beaufort, L., Barbarin, N., Gally, Y. (2014). Optical measurements to determine the thickness of calcite crystals and the mass of thin carbonate particles such as coccoliths. Nature Protocols, 9 (3), 633–642. doi: http://doi.org/10.1038/nprot.2014.028

Noor R. Al-Hasani*, Assistant Professor in Clinical Pharmacy, Department of Pharmacy, King's College London, Stamford str., 150, London, SE1 9NH, United Kingdom, Department of Basic Sciences, College of Dentistry, University of Baghdad, Bab-Almuadham, Baghdad, PO 1417, Iraq

Paul G. Royall, Senior Lecturer in Pharmaceutics, Department of Pharmacy, King's College London, Stamford str., 150, London, SE1 9NH, United Kingdom

Neil Rayment, Research Fellow, Department of Nutrition, King's College London, Stamford str., 150, London, SE1 9NH, United Kingdom

Kim Wolff, Professor of Analytical, Forensic and Addiction Science, King's Forensics, Department of Analytical Environmental & Forensic Science, King's College London, Stamford str., 150, London, SE1 9NH, United Kingdom

*Corresponding author: Noor R. Al-Hasani, e-mail: noor.al-hasani@kcl.ac.uk